Robust Iterative Learning Observers Based on a Combination of Stochastic Estimation Schemes and Ellipsoidal Calculus

Andreas Rauh
Department of Computing Science
Distributed Control in Interconnected Systems
Carl von Ossietzky Universität Oldenburg
Oldenburg, Germany
Andreas.Rauh@uni-oldenburg.de

Thomas Chevet
DTIS, ONERA
Université Paris-Saclay
Palaiseau, France
Thomas.Chevet@onera.fr

Thach Ngoc Dinh
Cedric-Laetitia
Conservatoire National des Arts et Métiers
Paris, France
ngoc-thach.dinh@lecnam.net

Julien Marzat
DTIS, ONERA
Université Paris-Saclay
Palaiseau, France
julien.marzat@onera.fr

Tarek Raïssi
Cedric-Laetitia
Conservatoire National des Arts et Métiers
Paris, France
tarek.raissi@cnam.fr

***Abstract*—The state estimation of repetitive processes with periodically repeated trajectories can be interpreted as the dual task of iterative learning control design. While the latter has been widely investigated over the last two decades, only few approaches exist for the design of iterative learning observers. However, the exploitation of the knowledge about periodically repeated trajectories, which occur among others in pick and place tasks in robotics as well as in charging and discharging of batteries, offers the opportunity to enhance the estimation accuracy from one execution of the control task to the next. In this paper, we generalize a linear stochastic approach for iterative learning state estimation, inspired by the Kalman filter in terms of a minimization of the estimation error covariance, to the class of models with bounded parameter uncertainty and to nonlinear ones that can be represented by means of quasi-linear discrete-time state-space representations. To solve this task, a novel combination of set-valued ellipsoidal state enclosure techniques with the aforementioned stochastic iterative learning state estimator is presented and visualized for a quasi-linear model of the charging/discharging dynamics of Lithium-Ion batteries.**

***Index Terms*—Iterative learning observers, Stochastic estimation, Repetitive processes, Ellipsoidal calculus**

I. Introduction

Two-dimensional (2D) systems are characterized by the fact that their state evolves both in the time domain and the iteration domain. Such system representations are widely used for the derivation and stability proof of iterative learning control (ILC) procedures [1]–[3]. In general, ILC aims at effectively enhancing the control accuracy of repetitive tasks when reference trajectories with a finite length are repeated periodically in each successive execution of the same control task. Moreover, it is typically also assumed in the frame of ILC that a reset of the system state to (nearly) identical initial conditions occurs at the beginning of each new iteration. Examples for scenarios in which ILC can outperform classical controllers by not only adjusting the control signal on the basis of state information from the current execution (also called iteration or trial), but also by accounting for tracking error signals from at least one previous trial, are pick and place operations in automated manufacturing processes, trajectory tracking for welding robots, rehabilitation robotics, or the control of wind power plants.

Iterative learning observer (ILO) synthesis [4] can be interpreted as the corresponding dual task. However, it is yet a quite novel direction of research, regardless of whether deterministic state observers, set-based estimation approaches, or stochastic filtering techniques are accounted for. As related research, especially the work by Cao et al. [5] should be mentioned, where a Kalman Filter (KF) [6] like ILO procedure is derived to account for the system dynamics in both the time and iteration domains. The drawback of this approach is its suboptimality due to the fact that both the time and iteration domains are treated independently. A first attempt to removing this problem was published in [7], where a robust linear matrix inequality (LMI) technique is presented that allows for a joint parameterization of the ILO gains in both domains. Although this ILO approach is robust against uncertain but bounded, possibly time-varying parameters, it only provides point-valued estimates for the system state. The structure of this observer is motivated by the work of [8]. Examples, in which nonlinear applications are taken into consideration by data-driven learning observer approaches can be found in [9], [10]. Recently, the authors have published a related work on the interval observer design for 2D systems described in the form of the Fornasini-Marchesini second model [11], where

the focus was on evaluating and verifying stability criteria in the form of LMIs in combination with the optimization of the peak-to-peak norm to reduce the effects of measurement errors on the state estimates. In addition, a KF-like realization of ILO was published in [12]. It aims at a minimization of the estimation error covariance by jointly tuning the filter gains in the time and iteration domains in a discrete-time setting. For nonlinear processes, it proposes a linearization of state and output equations in the most recent estimates for the expected values of a Gaussian approximation of the state's probability density as it is classically also being done in the synthesis of Extended Kalman Filters (EKFs).

To enhance the robustness of the KF-based ILO approach, a novel combination with a set-valued ellipsoidal calculus technique [13], [14] is presented in this paper. It aims at bounding the arising covariance matrices in both prediction and innovation stages after the specification of desired confidence levels for a quasi-linear state-space representation, i.e., for system and output matrices that may explicitly depend on the state and bounded parameters with unknown probability distributions. In such a way, the use of the ellipsoidal enclosure technique proposed in this paper can be seen as a generalization of the work in [15], where pure parameter uncertainties were accounted for in a time-domain (non-ILO) state estimation.

This paper is structured as follows. Sec. II summarizes the fundamental steps of the ellipsoidal calculus approach according to [13], [14] to form the basis for a novel technique to bound predicted covariances for quasi-linear system models. In Sec. III, we describe the problem formulation of ILO design for discrete-time, quasi-linear system models. Sec. IV proposes the generalization of the ILO design from [12] by the novel combination with the ellipsoidal bounding technique of Sec. II. The use of the ILO is demonstrated in simulations for a close-to-life battery model in Sec. V. Finally, conclusions and an outlook on future work can be found in Sec. VI.

II. Covariance Prediction Using Ellipsoidal Calculus

For the derivation of the application of the ellipsoidal calculus approach from [13], [14] to the prediction of covariance matrix bounds, assume that the discrete-time state-space model

$$\mathbf{z}_{k+1} = \mathbf{\Phi}\left(\mathbf{z}_k, \mathbf{p}\right) \cdot \mathbf{z}_k \tag{1}$$

with the bounded parameter vector $\mathbf{p} \in \left[\underline{\mathbf{p}}\,;\,\overline{\mathbf{p}}\right]$ — for which the elementwise defined relation $\underline{\mathbf{p}} \leq \overline{\mathbf{p}}$ holds — is given. As discussed further in Secs. III and IV, the vector $\mathbf{z}_k \in \mathbb{R}^{\tilde{n}}$ consists of both system states and noise variables. Furthermore, assume that an ellipsoidal domain

$$\begin{aligned}&\mathscr{E}_k\left(\boldsymbol{\mu}_k, \mathbf{\Gamma}'_k, r\right)\\ &:= \left\{\mathbf{z}_k \in \mathbb{R}^n \;\middle|\; \left(\mathbf{z}_k - \boldsymbol{\mu}_k\right)^T {\mathbf{\Gamma}'_k}^{-T} \mathbf{\Gamma}'_k{}^{-1} \left(\mathbf{z}_k - \boldsymbol{\mu}_k\right) \leq r^2\right\}\end{aligned} \tag{2}$$

is specified with the positive definite shape matrix $\mathbf{Q}'_k = \mathbf{\Gamma}'_k {\mathbf{\Gamma}'_k}^T \succ 0$ and the ellipsoid midpoint $\boldsymbol{\mu}_k \in \mathbb{R}^{\tilde{n}}$. The parameter r describes a magnification factor according to [16] so that the ellipsoid (2) specifies the confidence bound of a given percentage if the vector $\mathbf{z}_k$ is normally distributed with the covariance $\mathbf{Q}'_k$. For the cases $\tilde{n} = 4$ and $\tilde{n} = 8$ (inspired by the example in Sec. V), selected magnification factors r are listed in Tab. I.

TABLE I: Magnification factors for selected confidence levels for Gaussian distributions in different dimensions $\tilde{n}$ [16].

	confidence levels			
dimension	80%	85%	90%	95%
$\tilde{n} = 4$	2.4472	2.5971	2.7892	3.0802
$\tilde{n} = 8$	3.3212	3.4680	3.6553	3.9379

In the following ellipsoidal covariance prediction step, we use the definitions

$$\mathbf{\Gamma}_k := r \cdot \mathbf{\Gamma}'_k \quad \text{and} \quad \mathbf{Q}_k := r^2 \cdot \mathbf{Q}'_k \;. \tag{3}$$

The following procedure is based on the reference [14], from which only the computation of *outer* ellipsoidal bounds is taken into consideration.

For the compactness of notation, reformulate the system model (1) into the form

$$\mathbf{z}_{k+1} = \mathbf{\Phi}\left(\mathbf{z}_k, \mathbf{p}\right) \cdot \check{\mathbf{z}}_k + \tilde{\mathbf{\Phi}} \cdot \boldsymbol{\mu}_k + \left(\mathbf{\Phi}\left(\mathbf{z}_k, \mathbf{p}\right) - \tilde{\mathbf{\Phi}}\right) \cdot \boldsymbol{\mu}_k \tag{4}$$

with $\mathbf{z}_k = \check{\mathbf{z}}_k + \boldsymbol{\mu}_k$, where

$$\mathbf{z}_k \in \mathscr{E}_k = \mathscr{E}_k\left(\boldsymbol{\mu}_k, \mathbf{\Gamma}'_k, r\right) \;. \tag{5}$$

Here, $\mathscr{E}_k$ denotes the uncertainty on the non-origin centered states $\mathbf{z}_k$,

$$\check{\mathbf{z}}_k \in \check{\mathscr{E}}_k = \check{\mathscr{E}}_k\left(\mathbf{0}, \mathbf{\Gamma}'_k, r\right) \tag{6}$$

the uncertainty on $\check{\mathbf{z}}_k$ after shifting the ellipsoid to the origin, and

$$\tilde{\mathbf{\Phi}} = \mathbf{\Phi}\left(\boldsymbol{\mu}_k, \operatorname{mid}\left([\mathbf{p}]\right)\right) \tag{7}$$

is the midpoint approximation of the quasi-linear system matrix with

$$\operatorname{mid}\left([\mathbf{p}]\right) = \frac{1}{2} \cdot \left(\underline{\mathbf{p}} + \overline{\mathbf{p}}\right) \;. \tag{8}$$

Let also $\square\mathscr{E}_k$ denote an axis-aligned enclosure of $\mathscr{E}_k$ in the form of an $\tilde{n}$-dimensional interval box. An alternative to the definition (7) is given by

$$\tilde{\mathbf{\Phi}} = \operatorname{mid}\left(\mathbf{\Phi}\left(\square\mathscr{E}_k, [\mathbf{p}]\right)\right) \;, \tag{9}$$

which is preferable if (7) and (9) strongly differ from each other in the case of large uncertainty.

Then, a confidence bound of the predicted states $\mathbf{z}_{k+1}$ of magnification r is given by the ellipsoid $\mathscr{E}_{k+1}\left(\boldsymbol{\mu}_{k+1}, \mathbf{\Gamma}'_{k+1}, r\right)$ with the covariance $\mathbf{Q}'_{k+1} = \mathbf{\Gamma}'_{k+1}\left(\mathbf{\Gamma}'_{k+1}\right)^T$ for which the parameters are computed in the following steps.

P1: Apply

$$\check{\mathbf{z}}_{k+1} = \mathbf{\Phi}\left(\mathbf{z}_k, \mathbf{p}\right) \cdot \check{\mathbf{z}}_k \tag{10}$$

to the ellipsoid $\check{\mathscr{E}}_k$ in (6). The outer ellipsoid enclosure of the image set is described by an ellipsoid with the shape matrix

$$\check{\mathbf{Q}}_{k+1} = \alpha_{k+1}^2 \cdot \mathbf{\Gamma}_{k+1} \cdot \mathbf{\Gamma}_{k+1}^T \;, \tag{11}$$

where $\alpha_{k+1} \geq 0$ is the smallest value for which the LMI

$$\boldsymbol{\mathscr{M}}_{k+1} := \boldsymbol{\Lambda} \begin{bmatrix} -\mathbf{Q}_k^{-1} & \boldsymbol{\Phi}^T(\mathbf{z}_k, \mathbf{p}) \cdot \tilde{\boldsymbol{\Phi}}^{-T} \\ \tilde{\boldsymbol{\Phi}}^{-1} \cdot \boldsymbol{\Phi}(\mathbf{z}_k, \mathbf{p}) & -\alpha_{k+1}^2 \boldsymbol{\mathscr{R}}_k \end{bmatrix} \boldsymbol{\Lambda} \preceq 0 \tag{12}$$

is satisfied for all $\mathbf{z}_k \in \square\mathscr{E}_k$ and $\mathbf{p} \in [\mathbf{p}]$ with

$$\boldsymbol{\mathscr{R}}_k := \boldsymbol{\Gamma}_k \cdot \boldsymbol{\Gamma}_k^T \ . \tag{13}$$

In (12), the symbol $\preceq$ denotes the negative semi-definiteness of the corresponding matrix expression and $\boldsymbol{\Lambda} = \mathrm{blkdiag}\left(\beta \mathbf{I}_{\tilde{n}\times\tilde{n}}, \beta^{-1}\mathbf{I}_{\tilde{n}\times\tilde{n}}\right)$ is a preconditioning matrix defined with the help of the identity matrix $\mathbf{I}_{\tilde{n}\times\tilde{n}} \in \mathbb{R}^{\tilde{n}\times\tilde{n}}$ and the square root $\beta = \sqrt{\min\{\lambda_i(\mathbf{Q}_k)\}}$ of the smallest eigenvalue of $\mathbf{Q}_k$ as described in [17].

P2: Compute interval bounds for the term

$$\mathbf{b}_k = \left(\boldsymbol{\Phi}(\mathbf{p}) - \tilde{\boldsymbol{\Phi}}\right) \cdot \boldsymbol{\mu}_k \in [\mathbf{b}_k] \tag{14}$$

which accounts for a non-zero ellipsoid midpoint with $\mathbf{z}_k$, $\tilde{\boldsymbol{\Phi}}$, and $\mathbf{p}$ defined according to (5), (7), and (8). Inflate the ellipsoid bound described by the shape matrix (11) according to

$$\mathbf{Q}_{k+1} = (1 + \rho_{\mathrm{O},k+1})^2 \cdot \check{\mathbf{Q}}_{k+1} \ , \tag{15}$$

$$\rho_{\mathrm{O},k+1} = \sup\left\{\left\|\alpha_{k+1}^{-1} \cdot \boldsymbol{\Gamma}_k^{-1} \cdot [\mathbf{b}_k]\right\|\right\} \ . \tag{16}$$

For a definition of the interval-valued generalization of the Euclidean norm operator in (16), see [13].

P3: Compute the updated ellipsoid midpoint

$$\boldsymbol{\mu}_{k+1} = \tilde{\boldsymbol{\Phi}} \cdot \boldsymbol{\mu}_k \tag{17}$$

and its factorized shape matrix

$$\boldsymbol{\Gamma}'_{k+1} = \alpha_{k+1} \cdot (1 + \rho_{\mathrm{O},k+1}) \cdot \tilde{\boldsymbol{\Phi}} \cdot \boldsymbol{\Gamma}'_k \, . \tag{18}$$

Remark: For states that vary much slower than the considered discretization step size or the measurement sampling time, the scaling factors α_{k+1} and $\rho_{\mathrm{O},k+1}$ in (18) can be kept constant for a heuristically chosen number of subsequent time steps to reduce the cost related to the solution of (12). Note that this simplification (although not strictly producing outer ellipsoid bounds) is still more robust than a pure point-valued forecast of the covariance matrix in the following sections.

III. Problem Formulation: Stochastic ILO for Quasi-Linear State Equations

Consider the quasi-linear discrete-time state-space representation

$$\begin{aligned} \mathbf{x}_{k+1} &= \mathbf{A}(\mathbf{x}_k, \mathbf{p}) \cdot \mathbf{x}_k + \mathbf{E}(\mathbf{x}_k, \mathbf{p}) \cdot \mathbf{w}_k \\ \mathbf{y}_k &= \mathbf{C}(\mathbf{x}_k, \mathbf{p}) \cdot \mathbf{x}_k + \mathbf{v}_k \end{aligned} \tag{19}$$

with the state vector $\mathbf{x}_k \in \mathbb{R}^n$, the measured output vector $\mathbf{y}_k \in \mathbb{R}^m$ ($m \leq n$), as well as the uncorrelated process and measurement noise vectors $\mathbf{w}_k \in \mathbb{R}^{n_\mathbf{w}}$ and $\mathbf{v}_k \in \mathbb{R}^{n_\mathbf{v}}$, respectively. These noise vectors are both assumed to be normally distributed with the covariances $\mathbf{C}_{\mathbf{w},k}$ and $\mathbf{C}_{\mathbf{v},k}$ and vanishing mean. In this paper, an ILO procedure is designed to estimate the state vector $\mathbf{x}_k$ as well as its uncertainty (expressed by its covariance) by a KF-like procedure that does not only operate along the time domain k but also enhances the estimates from the trial i to the trial $i+1$. To allow for the identification of a systematic model mismatch, a lumped correction term $\boldsymbol{\delta}_k$ is added to the state equations (19) in the form

$$\mathbf{x}_{k+1} = \mathbf{A}(\mathbf{x}_k, \mathbf{p}) \cdot \mathbf{x}_k + \mathbf{E}(\mathbf{x}_k, \mathbf{p}) \cdot \mathbf{w}_k + \boldsymbol{\delta}_k \ . \tag{20}$$

In the following section, this estimation is implemented in a learning-type framework, in which the trials $\xi = i$ and $\xi = i+1$ are accounted for. In such a way, the actually measured data $\mathbf{y}_{\mathrm{m},k}^{\xi} = \mathbf{C}_k^{\xi} \cdot \mathbf{x}_k^{\xi} + \mathbf{v}_k^{\xi}$ correspond to the realizations of the general outputs $\mathbf{y}_k$ in (19) for both trials under investigation. In addition, the estimate for the temporal evolution of $\boldsymbol{\delta}_k$ is updated before starting the next trial.

Remark: In the system model (19), control inputs are not explicitly included. In this paper, the system inputs are assumed to be perfectly known, so that they do not influence the computation of covariance matrices in the following section but only lead to additive offsets on the state's expected values during the prediction step.

IV. Design of the Stochastic ILO Scheme

According to the previous section, process and measurement noise are assumed to be uncorrelated and normally distributed with zero mean. In the following, the superscript p denotes the result of the prediction step, while the superscript e refers to the estimation result as the outcome of the measurement-based innovation step.

A. Prediction Step

For the generalization of the ILO presented in [12] toward quasi-linear system models, we assume that the standard detectability requirement (also known for the KF synthesis) is satisfied. Moreover, we suppose that two gain matrices $\mathbf{H}_{1,k}^{i+1}$ and $\mathbf{H}_{2,k}^{i+1}$ are included in the observer, where the first one serves as a KF-like stabilization along the trial and the latter allows for reducing estimation errors between two subsequent trials. As a general index convention, the index i denotes the old trial for which state estimates already exist from the previous execution and $i+1$ denotes the current trial. To design the gains for the trial $i+1$, an augmented system model is employed that comprises the state equations of the models for both the i-th and $(i+1)$-st trials.

1) State- and Parameter-Dependent Disturbance Inputs $\mathbf{E}(\mathbf{x}_k, \mathbf{p})$: Define an ellipsoid for the augmented state vector

$$\mathbf{z}_k = \left[\left(\mathbf{x}_k^i\right)^T \quad \left(\mathbf{x}_k^{i+1}\right)^T \quad \left(\mathbf{w}_k^i\right)^T \quad \left(\mathbf{w}_k^{i+1}\right)^T\right]^T \tag{21}$$

corresponding to the result of the preceding innovation step, augmented by the influence of the uncorrelated process noise in both trials i and $i+1$ in the form

$$\mathscr{E}_k^{\mathrm{e},i|i+1}\left(\begin{bmatrix} \boldsymbol{\mu}_k^{\mathrm{e},i} \\ \boldsymbol{\mu}_k^{\mathrm{e},i+1} \\ \mathbf{0} \\ \mathbf{0} \end{bmatrix}, \boldsymbol{\Gamma}_k^{\mathrm{e}}, r\right) \tag{22}$$

with

$$\mathbf{\Gamma}_k^{\mathrm{e}} = \begin{bmatrix} \mathbf{\Gamma}_k^{\mathrm{e},i|i+1} & \mathbf{0}_{2n\times 2n_{\mathbf{w}}} \\ \mathbf{0}_{2n_{\mathbf{w}}\times 2n} & \begin{bmatrix} \mathbf{C}_{\mathbf{w},k} & \mathbf{0} \\ \mathbf{0} & \mathbf{C}_{\mathbf{w},k} \end{bmatrix}^{\frac{1}{2}} \end{bmatrix} \tag{23}$$

containing the matrix square root $\mathbf{\Gamma}_k^{\mathrm{e},i|i+1}$ of the combined state covariance matrix

$$\mathbf{C}_k^{\mathrm{e},i|i+1} = \mathbf{\Gamma}_k^{\mathrm{e},i|i+1} \cdot \left(\mathbf{\Gamma}_k^{\mathrm{e},i|i+1}\right)^T \tag{24}$$

as well as of the iteration-independent noise covariance $\mathbf{C}_{\mathbf{w},k}$, and the magnification factor $r \geq 1$ as a user-defined degree of freedom.

Then, the application of the system model

$$\mathbf{\Phi}\left(\mathbf{z}_k, \mathbf{p}\right) = \begin{bmatrix} \mathbf{A}\left(\mathbf{x}_k^i, \mathbf{p}\right) & \mathbf{0}_{n\times n} & \mathbf{E}\left(\mathbf{x}_k^i, \mathbf{p}\right) & \mathbf{0}_{n\times n_{\mathbf{w}}} \\ \mathbf{0}_{n\times n} & \mathbf{A}\left(\mathbf{x}_k^{i+1}, \mathbf{p}\right) & \mathbf{0}_{n\times n_{\mathbf{w}}} & \mathbf{E}\left(\mathbf{x}_k^{i+1}, \mathbf{p}\right) \\ \mathbf{0}_{n_{\mathbf{w}}\times n} & \mathbf{0}_{n_{\mathbf{w}}\times n} & \mathbf{I}_{n_{\mathbf{w}}\times n_{\mathbf{w}}} & \mathbf{0}_{n_{\mathbf{w}}\times n_{\mathbf{w}}} \\ \mathbf{0}_{n_{\mathbf{w}}\times n} & \mathbf{0}_{n_{\mathbf{w}}\times n} & \mathbf{0}_{n_{\mathbf{w}}\times n_{\mathbf{w}}} & \mathbf{I}_{n_{\mathbf{w}}\times n_{\mathbf{w}}} \end{bmatrix} \tag{25}$$

to the ellipsoid (22) according to Sec. II yields the ellipsoid

$$\mathscr{E}_{k+1}^{\mathrm{p},i|i+1}\left(\begin{bmatrix} \boldsymbol{\mu}_{k+1}^{\mathrm{p},i} \\ \boldsymbol{\mu}_{k+1}^{\mathrm{p},i+1} \\ \mathbf{0} \\ \mathbf{0} \end{bmatrix}, \mathbf{\Gamma}_{k+1}^{\mathrm{p}}, r\right) \tag{26}$$

in which the first $2n$ components of the midpoint represent the predicted expected value vector $\begin{bmatrix} \left(\boldsymbol{\mu}_{k+1}^{\mathrm{p},i}\right)^T & \left(\boldsymbol{\mu}_{k+1}^{\mathrm{p},i+1}\right)^T \end{bmatrix}^T$ and the covariance $\mathbf{C}_{k+1}^{\mathrm{p},i|i+1}$ is obtained by extracting the upper left $(2n \times 2n)$ block of the matrix product $\mathbf{\Gamma}_{k+1}^{\mathrm{p}} \cdot \left(\mathbf{\Gamma}_{k+1}^{\mathrm{p}}\right)^T$.

2) Constant (Parameter-Independent) Disturbance Inputs $\mathbf{E}$*:* For constant, i.e., state- and parameter independent disturbance inputs (which may however be varying in each discretization step), the following simplifications are possible for the augmented state vector

$$\mathbf{z}_k = \begin{bmatrix} \left(\mathbf{x}_k^i\right)^T & \left(\mathbf{x}_k^{i+1}\right)^T \end{bmatrix}^T \quad , \tag{27}$$

the ellipsoid of prior knowledge

$$\mathscr{E}_k^{\mathrm{e},i|i+1}\left(\begin{bmatrix} \boldsymbol{\mu}_k^{\mathrm{e},i} \\ \boldsymbol{\mu}_k^{\mathrm{e},i+1} \end{bmatrix}, \mathbf{\Gamma}_k^{\mathrm{e},i|i+1}, r\right) \quad , \tag{28}$$

and the augmented system model (25)

$$\mathbf{\Phi}\left(\mathbf{z}_k, \mathbf{p}\right) = \begin{bmatrix} \mathbf{A}\left(\mathbf{x}_k^i, \mathbf{p}\right) & \mathbf{0}_{n\times n} \\ \mathbf{0}_{n\times n} & \mathbf{A}\left(\mathbf{x}_k^{i+1}, \mathbf{p}\right) \end{bmatrix} \quad . \tag{29}$$

Then, the prediction result is the ellipsoid

$$\mathscr{E}_{k+1}^{\mathrm{p},i|i+1}\left(\begin{bmatrix} \boldsymbol{\mu}_{k+1}^{\mathrm{p},i} \\ \boldsymbol{\mu}_{k+1}^{\mathrm{p},i+1} \end{bmatrix}, \mathbf{\Gamma}_{k+1}^{\mathrm{p}}, r\right) \tag{30}$$

from which the forecasted covariance is obtained as

$$\begin{aligned} \mathbf{C}_{k+1}^{\mathrm{p},i|i+1} = \mathbf{\Gamma}_{k+1}^{\mathrm{p},i|i+1} \cdot \left(\mathbf{\Gamma}_{k+1}^{\mathrm{p},i|i+1}\right)^T &= \mathbf{\Gamma}_{k+1}^{\mathrm{p}} \cdot \left(\mathbf{\Gamma}_{k+1}^{\mathrm{p}}\right)^T \\ &+ \begin{bmatrix} \mathbf{E}_k^i & \mathbf{0} \\ \mathbf{0} & \mathbf{E}_k^{i+1} \end{bmatrix} \cdot \begin{bmatrix} \mathbf{C}_{\mathbf{w},k} & \mathbf{0} \\ \mathbf{0} & \mathbf{C}_{\mathbf{w},k} \end{bmatrix} \cdot \begin{bmatrix} \mathbf{E}_k^i & \mathbf{0} \\ \mathbf{0} & \mathbf{E}_k^{i+1} \end{bmatrix}^T . \end{aligned} \tag{31}$$

Remark: This prediction step becomes identical to the result of [12, Eqs. (4),(5)] if the system matrix $\mathbf{A}$ *is state-independent and only depends on precisely known point-valued parameters* $\mathbf{p}$*. Hence, our previous research is included as a special case in this more general formulation.*

B. Innovation Step

The measurement-based innovation step makes use of the deviations

$$\Delta\mathbf{y}_k^i = \mathbf{y}_{\mathrm{m},k}^i - \mathbf{C}_k^i \cdot \boldsymbol{\mu}_k^{\mathrm{p},i} \quad \text{and} \tag{32}$$

$$\Delta\mathbf{y}_k^{i+1} = \mathbf{y}_{\mathrm{m},k}^{i+1} - \mathbf{C}_k^{i+1} \cdot \boldsymbol{\mu}_k^{\mathrm{p},i+1} \tag{33}$$

between the measured data in the trials i and $i+1$, respectively, and the corresponding output forecasts based on the prediction step of the previous subsection. Using these output deviations, the expected values are updated according to [12] by

$$\begin{bmatrix} \boldsymbol{\mu}_k^{\mathrm{e},i} \\ \boldsymbol{\mu}_k^{\mathrm{e},i+1} \end{bmatrix} = \begin{bmatrix} \boldsymbol{\mu}_k^{\mathrm{p},i} \\ \boldsymbol{\mu}_k^{\mathrm{p},i+1} \end{bmatrix} + \tilde{\mathbf{H}}_k \cdot \begin{bmatrix} \mathbf{y}_{\mathrm{m},k}^i \\ \mathbf{y}_{\mathrm{m},k}^{i+1} \end{bmatrix} - \tilde{\mathbf{H}}_k \tilde{\mathbf{C}}_k \cdot \begin{bmatrix} \boldsymbol{\mu}_k^{\mathrm{p},i} \\ \boldsymbol{\mu}_k^{\mathrm{p},i+1} \end{bmatrix}, \tag{34}$$

where the combined output matrix

$$\tilde{\mathbf{C}}_k := \begin{bmatrix} \mathbf{C}_k^i & \mathbf{0} \\ \mathbf{0} & \mathbf{C}_k^{i+1} \end{bmatrix} \tag{35}$$

results from pointwise evaluations of the quasi-linear system's output matrix according to $\mathbf{C}_k^i := \mathbf{C}_k\left(\boldsymbol{\mu}_k^{\mathrm{p},i}, \mathrm{mid}\left([\mathbf{p}]\right)\right)$ and $\mathbf{C}_k^{i+1} := \mathbf{C}_k\left(\boldsymbol{\mu}_k^{\mathrm{p},i+1}, \mathrm{mid}\left([\mathbf{p}]\right)\right)$.

The corresponding estimation error covariance is given as

$$\begin{aligned} \mathbf{C}_k^{\mathrm{e},i|i+1} &= \mathrm{E}\left\{ \begin{bmatrix} \mathbf{x}_k^i - \boldsymbol{\mu}_k^{\mathrm{e},i} \\ \mathbf{x}_k^{i+1} - \boldsymbol{\mu}_k^{\mathrm{e},i+1} \end{bmatrix} \cdot \begin{bmatrix} \mathbf{x}_k^i - \boldsymbol{\mu}_k^{\mathrm{e},i} \\ \mathbf{x}_k^{i+1} - \boldsymbol{\mu}_k^{\mathrm{e},i+1} \end{bmatrix}^T \right\} \\ &= \mathrm{Cov}\left\{ \begin{bmatrix} \mathbf{x}_k^i - \boldsymbol{\mu}_k^{\mathrm{e},i} \\ \mathbf{x}_k^{i+1} - \boldsymbol{\mu}_k^{\mathrm{e},i+1} \end{bmatrix} \right\} \\ &= \mathbf{M}_k \mathbf{C}_k^{\mathrm{p},i|i+1} \mathbf{M}_k^T + \tilde{\mathbf{H}}_k \tilde{\mathbf{C}}_{\mathbf{v},k} \tilde{\mathbf{H}}_k^T \quad , \end{aligned} \tag{36}$$

where

$$\mathbf{M}_k = \begin{bmatrix} \mathbf{I} & \mathbf{0} \\ \mathbf{0} & \mathbf{I} \end{bmatrix} - \tilde{\mathbf{H}}_k \tilde{\mathbf{C}}_k \quad \text{and} \tag{37}$$

$$\tilde{\mathbf{H}}_k := \begin{bmatrix} \mathbf{H}_{1,k}^{i+1} & \mathbf{0} \\ \mathbf{H}_{2,k}^{i+1} & \mathbf{H}_{1,k}^{i+1} - \mathbf{H}_{2,k}^{i+1} \end{bmatrix} \quad . \tag{38}$$

As shown in [12], the estimation error covariance is minimized by the filter gain matrices $\mathbf{H}_{1,k}^{i+1}$ and $\mathbf{H}_{2,k}^{i+1}$ specified in the following Theorem 4.1 in which the predicted covariance is partitioned in a blockwise manner according to

$$\mathbf{C}_k^{\mathrm{p},i|i+1} = \begin{bmatrix} \mathbf{C}_{\mathrm{A},k}^{\mathrm{p}} & \mathbf{C}_{\mathrm{B},k}^{\mathrm{p}} \\ \star & \mathbf{C}_{\mathrm{C},k}^{\mathrm{p}} \end{bmatrix} \quad , \tag{39}$$

where $\star$ denotes blocks that can be inferred from the symmetry of the result. Moreover, the residual covariance is defined as

$$\mathbf{P} \cdot \tilde{\mathbf{\Gamma}}_k^{\mathrm{e}} \cdot \left(\tilde{\mathbf{\Gamma}}_k^{\mathrm{e}}\right)^T \cdot \mathbf{P}^T + \tilde{\mathbf{C}}_{\mathbf{v},k} = \begin{bmatrix} \mathbf{C}_{\mathrm{A},k} & \mathbf{C}_{\mathrm{B},k} \\ \star & \mathbf{C}_{\mathrm{C},k} \end{bmatrix} \tag{40}$$

with the projection matrix $\mathbf{P} = \begin{bmatrix} \mathbf{I}_{m\times m} & \mathbf{0}_{m\times(n-m)} \end{bmatrix}$ and the trial-independent measurement noise covariance

$$\tilde{\mathbf{C}}_{\mathbf{v},k} := \begin{bmatrix} \mathbf{C}_{\mathbf{v},k} & \mathbf{0} \\ \mathbf{0} & \mathbf{C}_{\mathbf{v},k} \end{bmatrix} \quad . \tag{41}$$

As a novel feature of this paper, aiming at a robustification of the innovation stage against nonlinearities, the matrix $\tilde{\mathbf{\Gamma}}_k^{\mathrm{e}}$ is obtained by the consideration of the quasi-linearity of the output equation with the help of the ellipsoid

$$\mathscr{E}_k^{\mathrm{p},i|i+1}\left(\begin{bmatrix}\boldsymbol{\mu}_k^{\mathrm{p},i}\\ \boldsymbol{\mu}_k^{\mathrm{p},i+1}\end{bmatrix}, \mathbf{\Gamma}_k^{\mathrm{p},i|i+1}, r\right) \tag{42}$$

as the one time step delayed version of (31) that is propagated through a quasi-linear system model in the form (1) with the associated system matrix ($\mathbf{y}_{\mathrm{m},k}^i, \mathbf{y}_{\mathrm{m},k}^{i+1} \in \mathbb{R}^m$)

$$\mathbf{\Phi}\left(\mathbf{z}_k, \mathbf{p}\right) = \begin{bmatrix} \mathbf{C}\left(\mathbf{x}_k^i, \mathbf{p}\right) & \mathbf{0}_{m\times n} \\ \mathbf{0}_{m\times n} & \mathbf{C}\left(\mathbf{x}_k^{i+1}, \mathbf{p}\right) \\ \mathbf{0}_{(n-m)\times m} \quad \mathbf{I}_{(n-m)\times(n-m)} & \mathbf{0}_{(n-m)\times n} \\ \mathbf{0}_{(n-m)\times n} & \mathbf{0}_{(n-m)\times m} \quad \mathbf{I}_{(n-m)\times(n-m)} \end{bmatrix}, \tag{43}$$

where $\mathbf{\Phi}\left(\mathbf{z}_k, \mathbf{p}\right) \in \mathbf{R}^{2n\times 2n}$. The evaluation of this quasi-linear model yields an ellipsoid

$$\mathscr{E}_k^{\mathrm{e}}\left(\tilde{\boldsymbol{\mu}}_k^{\mathrm{e}}, \tilde{\mathbf{\Gamma}}_k^{\mathrm{e}}, r\right) \tag{44}$$

from which the associated shape matrix $\tilde{\mathbf{\Gamma}}_k^{\mathrm{e}} \cdot \left(\tilde{\mathbf{\Gamma}}_k^{\mathrm{e}}\right)^T$ is computed in Eq. (40), followed by an extraction of the upper left $(2m \times 2m)$ block that corresponds to the actually measured output quantities. This subblock extraction is performed by the multiplication with the projection matrix $\mathbf{P}$ in the first summand of Eq. (40).

Remark: This procedure is based on the assumption that cross-correlations between the trials i and $i+1$ due to the stochastic noise are negligible.

Theorem 4.1 (Optimal ILO gain computation): The optimal ILO gains, in the sense of a minimization of the estimation error covariance, jointly considering the trials i and $i+1$ are given by

$$\begin{bmatrix} \mathbf{H}_{1,k}^{i+1} \mid \mathbf{H}_{2,k}^{i+1} \end{bmatrix} = \left[\left(\mathbf{C}_k^i \mathbf{C}_{\mathrm{A},k}^{\mathrm{p}} + \mathbf{C}_k^{i+1}\mathbf{C}_{\mathrm{C},k}^{\mathrm{p}}\right)^T \middle| \left(\mathbf{C}_k^i \mathbf{C}_{\mathrm{B},k}^{\mathrm{p}} - \mathbf{C}_k^{i+1}\mathbf{C}_{\mathrm{C},k}^{\mathrm{p}}\right)^T\right] \cdot \begin{bmatrix} \mathbf{C}_{\mathrm{A},k} + \mathbf{C}_{\mathrm{C},k} & \star \\ \mathbf{C}_{\mathrm{B},k} - \mathbf{C}_{\mathrm{C},k} & \mathbf{C}_{\mathrm{A},k} - \left(\mathbf{C}_{\mathrm{B},k} + \mathbf{C}_{\mathrm{B},k}^T\right) + \mathbf{C}_{\mathrm{C},k} \end{bmatrix}^{-1}. \tag{45}$$

For a proof of this expression for the ILO filter gain matrices, see [12].

C. Summary of the ILO Procedure

As shown in the previous two subsections, an ellipsoidal calculus can be used to implement the prediction and innovation stages of the stochastic ILO procedure in the case of quasi-linear system models. So far, the description was focused on the update from trial i to trial $i+1$. During the very first trial $i = 0$, the only required change is to remove the rows and columns for the trial $i+1$ from the expressions (25), (29), and (43) so that pure along-the-trial dynamics are taken into consideration in this phase. Moreover, it is necessary to correct the state estimates from trial to trial by storing the lumped correction term $\boldsymbol{\delta}_k^i$ introduced in Eqs. (20) and (47), see also Fig. 1.

V. Benchmark Example

A. Modeling of the Charging/ Discharging Dynamics of Lithium-Ion Batteries

Equivalent circuit models of Lithium-Ion batteries as shown in Fig. 2 (cf. [18]–[20]) are widely used to approximate their charging/discharging dynamics. For such models, the state variables are chosen as the normalized state of charge (SOC) $\sigma(t)$ as well as the voltages across a finite number of RC sub-networks. In this paper, we restrict ourselves to the case of two RC sub-networks with the voltages $v_{\mathrm{TL}}(t)$ and $v_{\mathrm{TS}}(t)$ to distinguish processes with short and large time constants (TS and TL, respectively). They result from electro-chemical polarization effects and concentration losses during charging and discharging.

With the help of the state vector

$$\mathbf{x}(t) = \begin{bmatrix}\sigma(t) & v_{\mathrm{TS}}(t) & v_{\mathrm{TL}}(t) & i_{\mathrm{T}}(t)\end{bmatrix}^T \ , \tag{48}$$

the quasi-linear, continuous-time battery model is given as

$$\dot{\mathbf{x}}(t) = \mathbf{A}\left(\sigma(t)\right)\cdot\mathbf{x}(t) + \mathbf{b}\cdot u(t) = \begin{bmatrix} 0 & 0 & 0 & \frac{-1}{C_{\mathrm{Bat}}} \\ 0 & \frac{-1}{C_{\mathrm{TS}}\cdot R_{\mathrm{TS}}} & 0 & \frac{1}{C_{\mathrm{TS}}} \\ 0 & 0 & \frac{-1}{C_{\mathrm{TL}}\cdot R_{\mathrm{TL}}} & \frac{1}{C_{\mathrm{TL}}} \\ 0 & 0 & 0 & \frac{-1}{T_{\mathrm{I}}} \end{bmatrix}\cdot\mathbf{x}(t) + \begin{bmatrix}0\\0\\0\\\frac{1}{T_{\mathrm{I}}}\end{bmatrix}\cdot u(t) \tag{49}$$

in which the terminal current results from a fast controller with the linear first-order lag behavior ($T_{\mathrm{I}} = 0.1\,\mathrm{s}$)

$$T_{\mathrm{I}}\cdot\frac{\mathrm{d}i_{\mathrm{T}}(t)}{\mathrm{d}t} + i_{\mathrm{T}}(t) = i_{\mathrm{d}}(t) \ . \tag{50}$$

In (50), the set-point for this current controller represents the system input $u(t) := i_{\mathrm{d}}(t)$.

In detail, the model according to Eq. (49) consists of the integrating behavior

$$\dot{\sigma}(t) = -\frac{i_{\mathrm{T}}(t)}{C_{\mathrm{Bat}}} \tag{51}$$

between the terminal current and the normalized SOC $\sigma(t) \in [0\ ;\ 1]$. Here, $\sigma = 1$ corresponds to the fully charged battery with the capacitance C_{Bat} and $\sigma = 0$ represents the completely discharged battery. Moreover, the differential equations [18], [19]

$$\dot{v}_\iota(t) = \frac{-v_\iota(t)}{C_\iota(t)\cdot R_\iota(t)} + \frac{i_{\mathrm{T}}(t)}{C_\iota(t)} \tag{52}$$

with the SOC-dependent parameters

$$R_\iota(t) = R_{\iota\mathrm{a}}\cdot e^{R_{\iota\mathrm{b}}\cdot\sigma(t)} + R_{\iota\mathrm{c}} \ , \tag{53}$$

$$C_\iota(t) = C_{\iota\mathrm{a}}\cdot e^{C_{\iota\mathrm{b}}\cdot\sigma(t)} + C_{\iota\mathrm{c}} \ , \quad \iota \in \{\mathrm{TS}, \mathrm{TL}\} \ , \tag{54}$$

as identified experimentally in [21], describe the battery dynamics in transient operating phases.

Set $i = 0$, $k = 0$

Define the magnification factor r for the desired confidence level in the ellipsoidal calculus

While $k < k_{\max}$

- **Evaluate** the state and covariance prediction $(\boldsymbol{\mu}_{k+1}^{\mathrm{p},0}, \mathbf{C}_{k+1}^{\mathrm{p},0})$ with the help of the quasi-linear models (25) or (29) after removing the entries for $i+1$
- **Compute** the Kalman gain $\mathbf{H}_{1,k}^{0}$ similar to a standard (E)KF procedure, where the residual covariance is computed with the help of (40), again after removing the iteration $i+1$
- **Evaluate** the state update in the innovation step: $\boldsymbol{\mu}_k^{\mathrm{e},0} = \boldsymbol{\mu}_k^{\mathrm{p},0} + \mathbf{H}_{1,k}^{0} \cdot \left(\mathbf{y}_{\mathrm{m},k}^{0} - \mathbf{C}_k \boldsymbol{\mu}_k^{\mathrm{p},0} \right)$
- **Evaluate** the covariance update in the innovation step by the standard (E)KF procedure
- **Set** $k := k+1$

Set $\boldsymbol{\delta}_k^0 = \mathbf{0}$ for all $k \in \{0, \ldots, k_{\max}\}$

Store the measurement sequence $\mathbf{y}_{\mathrm{m},k}^{0}$

While $i < i_{\max}$

- **Set** $k = 0$
- **While** $k < k_{\max}$
  - **Evaluate** the state prediction by adding the offset vector
    $$\begin{bmatrix} \boldsymbol{\delta}_k^i \\ \boldsymbol{\delta}_k^i \end{bmatrix} \tag{46}$$
    to the the quasi-linear models (25) or (29) and update the covariance according to (26) and (31), resp.
  - **Compute** the optimal ILO gain acc. to Theorem 4.1
  - **Evaluate** the state and covariance update in the innovation step acc. to Eqs. (34) and (36)
  - **Set** $k := k+1$
- **Update**
  $$\boldsymbol{\delta}_k^{i+1} = \left((i-1) \cdot \boldsymbol{\delta}_k^i + \mathbf{H}_{2,k}^{i+1} \cdot \left(\Delta \mathbf{y}_k^i - \Delta \mathbf{y}_k^{i+1} \right) \right) \cdot \tfrac{1}{i} \tag{47}$$
- **Increment** the trial counter $i := i+1$
- **Store** the measurement sequence $\mathbf{y}_{\mathrm{m},k}^{i}$

Fig. 1: Structure diagram of the complete stochastic ILO algorithm using ellipsoidal calculus for the computation of covariance matrices.

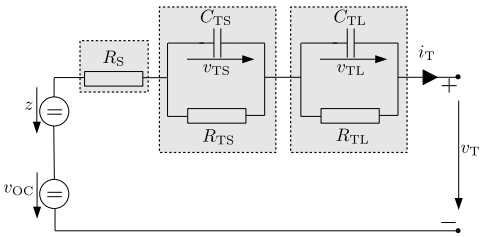

Fig. 2: Equivalent circuit model of a Lithium-Ion battery, where the special case of the disturbance voltage $z = 0$ is treated in this paper.

With the help of Kirchhoff's voltage law

$$v_{\mathrm{T}}(t) = v_{\mathrm{OC}}(t) - v_{\mathrm{TS}}(t) - v_{\mathrm{TL}}(t) - i_{\mathrm{T}}(t) \cdot R_{\mathrm{S}}(t) \ , \tag{55}$$

where

$$R_{\mathrm{S}}(t) = R_{\mathrm{Sa}} \cdot e^{R_{\mathrm{Sb}} \cdot \sigma(t)} + R_{\mathrm{Sc}} \tag{56}$$

is the SOC-dependent series resistance, the battery's terminal voltage can be determined as the second measurable system output besides the terminal current $i_{\mathrm{T}}(t)$. In (55), the open-circuit voltage of the battery is included in the form

$$v_{\mathrm{OC}}(\sigma(t)) = v_0 \cdot e^{v_1 \cdot \sigma(t)} + \sum_{i=0}^{3} v_{i+2} \cdot \sigma^i(t) \ , \tag{57}$$

where the parameters are again identified experimentally in [21]. To turn Eq. (57) into a quasi-linear form, the state-independent offset terms are subtracted from the expression for the open-circuit voltage so that the expression

$$\begin{aligned} \tilde{v}_{\mathrm{OC}}(\sigma(t)) &= \eta_{\mathrm{OC}}\left(\sigma(t)\right) \cdot \sigma(t) = v_{\mathrm{OC}}(\sigma(t)) - v_0 - v_2 \\ &= \left(v_0 \cdot \frac{e^{v_1 \cdot \sigma(t)} - 1}{\sigma(t)} + v_3 + v_4 \cdot \sigma(t) + v_5 \cdot \sigma^2(t) \right) \cdot \sigma(t) \end{aligned} \tag{58}$$

is obtained. In combination with the current measurement, this leads to the vector-valued output equation

$$\mathbf{y}(t) = \begin{bmatrix} i_{\mathrm{T}}(t) \\ \tilde{v}_{\mathrm{T}}(t) \end{bmatrix} = \begin{bmatrix} i_{\mathrm{T}}(t) \\ \tilde{v}_{\mathrm{OC}}(t) - v_{\mathrm{TS}}(t) - v_{\mathrm{TL}}(t) - i_{\mathrm{T}}(t) \cdot R_{\mathrm{S}}(t) \end{bmatrix} \tag{59}$$

with the associated quasi-linear representation

$$\begin{aligned} \mathbf{y}(t) &= \mathbf{C}\left(\sigma(t)\right) \cdot \mathbf{x}(t) \\ &= \begin{bmatrix} 0 & 0 & 0 & 1 \\ \eta_{\mathrm{OC}}\left(\sigma(t)\right) & -1 & -1 & -R_{\mathrm{S}}(t) \end{bmatrix} \cdot \mathbf{x}(t) \ . \end{aligned} \tag{60}$$

A temporally discretized version

$$\mathbf{x}_{k+1} = \mathbf{A}\left(\mathbf{x}_k, \mathbf{p}\right) \cdot \mathbf{x}_k + \mathbf{b}_k u_k + \mathbf{w}_k \tag{61}$$

following the formulation in (19) is obtained by the explicit Euler discretization

$$\mathbf{A}\left(\mathbf{x}_k, \mathbf{p}\right) = \mathbf{I}_{4\times 4} + T \cdot \mathbf{A}\left(\sigma(t_k)\right) \ , \tag{62}$$

where $\mathbf{x}_k := \mathbf{x}(t_k)$, with the sufficiently small step size T (here: $T = 10\,\mathrm{ms}$), $\mathbf{E} = \mathbf{I}_{4\times 4}$, the input term

$$\mathbf{b}_k u_k = T \cdot \mathbf{b} \cdot u(t_k) \ , \tag{63}$$

and the normally distributed process noise vector $\mathbf{w}_k$.

For the output equation, the relation $\mathbf{C}\left(\mathbf{x}_k, \mathbf{p}\right) = \mathbf{C}\left(\sigma(t_k)\right)$ holds in the quasi-linear system model (19). As described in Fig. 1, an additive correction term $\boldsymbol{\delta}_k^i$ is included in the ILO procedure to account for estimates of a potential model mismatch. During the following simulation-based validation of the proposed ILO approach, the covariance matrices of process and measurement noise are set to

$$\mathbf{C}_{\mathbf{w},k} = 0.01^2 \cdot \mathbf{I}_{4\times 4} \quad \text{and} \quad \mathbf{C}_{\mathbf{v},k} = \begin{bmatrix} 0.01 & 0 \\ 0 & 100 \end{bmatrix} . \quad (64)$$

In contrast to [12], where the resistances, capacitances, and further coefficients in (50), (51), (53), (54), (56), and (57) were assumed to be known in the ILO's prediction and innovation stages, the ellipsoidal calculus in Secs. IV-A and IV-B replaces these quantities by tolerance bounds of $\pm 2\,\%$ around their nominal values listed in [21] with additionally making sure that the interval bounds for the SOC in the system and output matrices are always limited to the maximum range $[0.01\ ;\ 0.99]$ (to avoid an extrapolation of the SOC-dependent characteristics into a physically meaningless area).

B. Simulation Results of the ILO Approach

To make the simulation results for the extended ILO algorithm derived in this paper comparable with the fundamental version published in [12], the same two cases of a model-mismatch are considered:

C1: The true system, generating the measured data, has an additive offset $\begin{bmatrix} -10^{-8} & 0 & 10^{-4} & 0 \end{bmatrix}^T$ in comparison with the state Eqs. (49), representing errors in the magnitude of 0.02% wrt. the charging efficiency and up to 300% in the variation rates of the voltage v_{TL}.

C2: In addition to the error of **C1**, all non-zero elements of the discretized system matrix in (62) are disturbed by independent time-invariant factors $1+d$ for the generation of the simulated measurements, where all d are uniformly distributed random numbers from the interval $[0\ ;\ 0.1]$.

In all simulations shown in Figs. 3 and 4, the true initial state (unknown to the ILO) is set to $\mathbf{x}(0) = \begin{bmatrix} 0.65 & 0 & 0 & 0 \end{bmatrix}^T$ with the ILO initialization $\boldsymbol{\mu}_0^{\mathrm{e},0} = \begin{bmatrix} 0.78 & 0 & 0 & 0 \end{bmatrix}^T$ and $u(t) = 2\,\mathrm{A}\sin(2\pi t \cdot 3600\mathrm{s}^{-1})$. For the evaluation of the ellipsoidal covariance prediction, the magnification factors r in Tab. I were chosen for the confidence level of 80% with $\tilde{n} = 4$ for the iteration $i = 0$ and $\tilde{n} = 8$ for $i \geq 1$.

Fig. 3 gives a comparison of the EKF-based implementation published in [12] with the novel ellipsoidal covariance prediction approach for the **Case C1**. It can be seen clearly that the new approach outperforms the original version by producing much tighter uncertainty bounds by an enhanced handling of the nonlinearities in the state and output equations of the system model. Exemplarily, estimation errors for the SOC σ and the voltage v_{TS} are visualized in this figure. This enhancement is already visible in the iteration $i = 0$ (the classical state estimation without iterative learning behavior).

Note that the superior estimation performance of the new implementation is confirmed also for the **Case C2** in Fig. 4, where the remaining two state variables are depicted. In all cases under consideration, the proposed estimator produces estimates for which (except for small values of time), the true states are included in a ± 1 standard deviation bound around the computed expected values.

VI. Conclusions and Outlook on Future Work

In this paper, a new combination of an ellipsoidal enclosure approach with stochastic state estimation was presented for the design of ILO approaches. Besides the visualized improved efficiency and robustness of the new implementation, in comparison with an EKF-like handling of nonlinearities, the new approach can also handle bounded parameter uncertainty without the need to include them as additional variables in the state or noise vectors. Typically, process and measurement noise covariances can be chosen smaller due to this property than for a classical parameterization because state and bounded parameter dependencies in the system and output matrices are already accounted for by the ellipsoidal enclosure approach.

Future work will especially focus on extensions that also allow for identifying the initial system states more accurately if they are imprecisely known but can be assumed to have the same value at the beginning of each subsequent trial. Moreover, optimization approaches will be developed that allow for not only taking into account the output errors (32) and (33) for the state estimation but also larger windows of measured data from one or multiple previous trials.

References

[1] S. Arimoto, S. Kawamura, and F. Miyazaki, "Bettering Operations of Robots by Learning," *Journal of Robotic Systems*, vol. 1, no. 1, pp. 123–140, 1984.

[2] H. S. Ahn, Y. Chen, and K. L. Moore, "Iterative Learning Control: Brief Survey and Categorization," *IEEE Transactions on Systems, Man and Cybernetics, Part C*, vol. 37, no. 6, pp. 1109–1121, 2007.

[3] D. A. Bristow, M. Tharayil, and A. G. Alleyne, "A survey of iterative learning control: A learning-based method for high-performance tracking control," *IEEE Control Systems Magazine*, vol. 26, no. 3, pp. 96–114, 2006.

[4] J. Hatonen and K. L. Moore, "A New Arimoto-Type Algorithm to Estimate States for Repetitive Processes: Iterative Learning Observer (ILO)," in *Proc. of 22nd Intl. Symposium on Intelligent Control*, Singapore, 2007, pp. 232–236.

[5] Z. Cao, J. Lu, R. Zhang, and F. Gao, "Iterative Learning Kalman Filter for Repetitive Processes," *Journal of Process Control*, vol. 46, pp. 92–104, 2016.

[6] R. Kalman, "A New Approach to Linear Filtering and Prediction Problems," *Transaction of the ASME – Journal of Basic Engineering*, vol. 82, no. Series D, pp. 35–45, 1960.

[7] A. Rauh, J. Kersten, and H. Aschemann, "Iterative Learning Approaches for Discrete-Time State and Disturbance Observer Design of Uncertain Linear Parameter-Varying Systems," in *Proc. of the 8th IFAC Symposium on Mechatronic Systems MECHATRONICS 2019*, Vienna, Austria, 2019.

[8] W. Chen and M. Saif, "An Iterative Learning Observer-Based Approach to Fault Detection and Accommodation in Nonlinear Systems," in *Proc. of the 40th IEEE Conference on Decision and Control*, vol. 5, Orlando, FL, USA, 2001, pp. 4469–4474.

[9] A. Chakrabarty, A. Zemouche, R. Rajamani, and M. Benosman, "Robust Data-Driven Neuro-Adaptive Observers With Lipschitz Activation Functions," in *Proc. of the 58th Conference on Decision and Control (CDC)*, Nice, France, 2019, pp. 2862–2867.

[10] A. Chakrabarty and M. Benosman, "Safe Learning-based Observers for Unknown Nonlinear Systems using Bayesian Optimization," 2021, https://arxiv.org/abs/2005.05888.

[11] T. Chevet, A. Rauh, T. N. Dinh, J. Marzat, and T. Raïssi, "Robust Interval Observer for Systems Described by the Fornasini-Marchesini Second Model," *IEEE Control Systems Letters*, vol. 6, pp. 1940–1945, 2022.

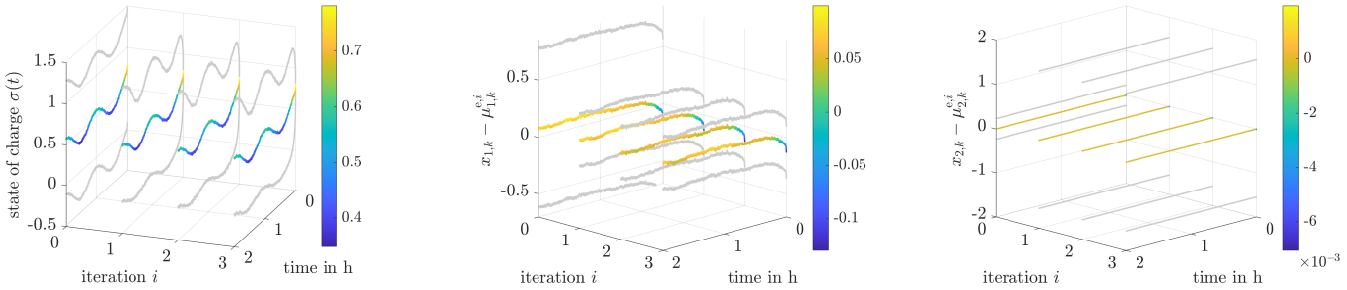

(a) Estimation of the SOC σ. (b) Estimation error of the SOC σ. (c) Estimation error of the voltage v_{TS}.

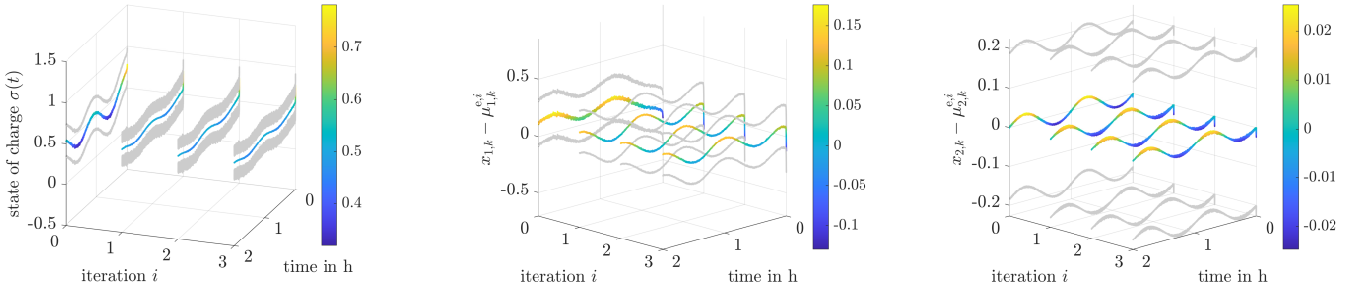

(d) Estimation of the SOC σ. (e) Estimation error of the SOC σ. (f) Estimation error of the voltage v_{TS}.

Fig. 3: Estimation results of the stochastic ILO in the **Case C1** with ± 1 standard deviation bounds in gray color (EKF-based version of [12] in Figs. 3a–3c; new ellipsoidal covariance prediction in Figs. 3d–3f).

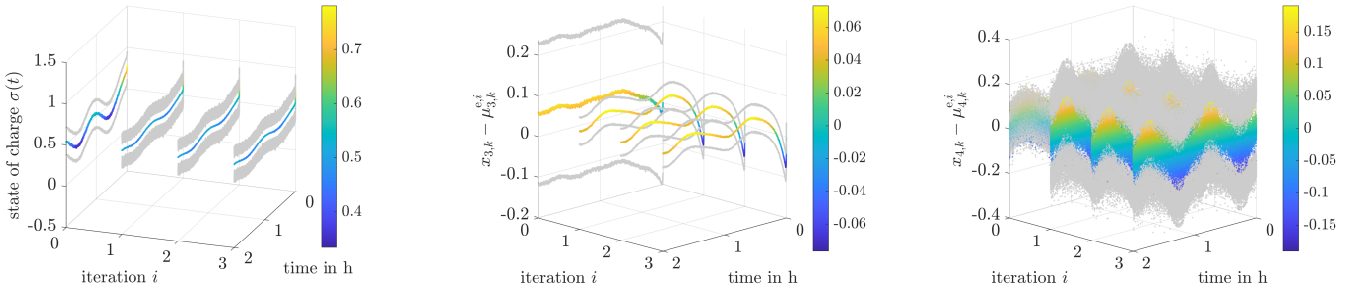

(a) Estimation of the SOC σ. (b) Estimation error of the voltage v_{TL}. (c) Estimation error of the current i_{TS}.

Fig. 4: Estimation results of the stochastic ILO in the **Case C2** with ± 1 standard deviation bounds in gray color (new ellipsoidal covariance prediction), where the iteration 0 corresponds to the pure along-the-trial estimates.

[12] A. Rauh, T. Chevet, T. N. Dinh, J. Marzat, and T. Raïssi, "A Stochastic Design Approach for Iterative Learning Observers for the Estimation of Periodically Recurring Trajectories and Disturbances," in *Proc. of the 20th European Control Conference ECC*, London, UK, 2022.

[13] A. Rauh and L. Jaulin, "A Computationally Inexpensive Algorithm for Determining Outer and Inner Enclosures of Nonlinear Mappings of Ellipsoidal Domains," *International Journal of Applied Mathematics and Computer Science AMCS*, vol. 31, no. 3, pp. 399–415, 2021.

[14] A. Rauh, A. Bourgois, and L. Jaulin, "Union and Intersection Operators for Thick Ellipsoid State Enclosures: Application to Bounded-Error Discrete-Time State Observer Design," *Algorithms*, vol. 14, no. 3, p. 88, 2021.

[15] T. A. Tran, C. Jauberthie, L. Travé-Massuyès, and Q. H. Lu, "Interval Kalman Filter Enhanced by Lowering the Covariance Matrix Upper Bound," *International Journal of Applied Mathematics and Computer Science AMCS*, vol. 31, no. 2, pp. 259–269, 2021.

[16] B. Wang, W. Shi, and Z. Miao, "Confidence Analysis of Standard Deviational Ellipse and Its Extension into Higher Dimensional Euclidean Space," *PLOS ONE*, vol. 10, no. 3, pp. 1–17, 03 2015.

[17] A. Rauh, A. Bourgois, L. Jaulin, and J. Kersten, "Ellipsoidal Enclosure Techniques for a Verified Simulation of Initial Value Problems for Ordinary Differential Equations," in *Proc. of 5th International Conference on Control, Automation and Diagnosis (ICCAD'21)*, Grenoble, France, 2021.

[18] O. Erdinc, B. Vural, and M. Uzunoglu, "A Dynamic Lithium-Ion Battery Model Considering the Effects of Temperature and Capacity Fading," in *Proceedings of International Conference on Clean Electrical Power*, 2009, pp. 383–386.

[19] A. Rauh, S. Butt, and H. Aschemann, "Nonlinear State Observers and Extended Kalman Filters for Battery Systems," *International Journal of Applied Mathematics and Computer Science AMCS*, vol. 23, no. 3, pp. 539–556, 2013.

[20] L. Senkel, A. Rauh, and H. Aschemann, "Robust Procedures for the Estimation of Operating Conditions of Lithium-Ion Battery Cells," in *Proc. of 2nd Intl. Conference on Control and Fault-Tolerant Systems (SysTol)*, Nice, France, 2013.

[21] J. Reuter, E. Mank, H. Aschemann, and A. Rauh, "Battery State Observation and Condition Monitoring Using Online Minimization," in *Proc. of 21st Intl. Conference on Methods and Models in Automation and Robotics*, Miedzyzdroje, Poland, 2016.